The GPS Block IIR Antenna Panel Pattern and Its Use On-Orbit

Willard Marquis
Lockheed Martin Space Systems Company

BIOGRAPHY

Willard Marquis is the GPS IIR/IIR-M Chief Engineer on the GPS Block IIR/IIR-M and GPS III Flight Operations Group in Colorado Springs, CO. He has a Bachelors Degree and a Masters Degree in Aeronautics and Astronautics from the Massachusetts Institute of Technology. He has worked at Lockheed Martin since 1982 on several rocket, upper stage and satellite programs. In 1994, he joined the GPS IIR Group at Schriever AFB.

ABSTRACT

The Global Positioning System Block IIR space vehicles on-orbit consists of the 12 original 'classic' IIR SVs and the eight 'modernized' IIR-M SVs. Lockheed Martin, as a stepping-stone toward the IIR-M modernization, developed and deployed an updated version of the satellite antenna panel for the L-band broadcast signal. This is the Earth-pointing signal. This paper is the first public presentation of the antenna panel patterns for these two versions.

This paper also presents design descriptions of both antenna panel versions, their broadcast signal patterns, the performance observed in factory testing, and their on-orbit performance. The antenna pattern out to +/- 90 degrees will be presented, covering the terrestrial service as well as the space service. All users, both terrestrial and on-orbit, benefit from the enhanced power profile of the GPS IIR and IIR-M antennas. The IIR and IIR-M SVs have shown great benefit to the space user in recent years. Some of these benefits will be presented. Specifically, the on-orbit use of these patterns by NASA, ESA, and other missions will be examined.

INTRODUCTION

The Global Positioning System (GPS) Block II Replenishment (IIR) space vehicle (SV) began improving upon its baseline design in 2003 with the launch of the first Block IIR SV retrofitted with a re-designed 'improved' antenna panel [1]. This is the Earth-facing panel providing the GPS L-band broadcast signal. This improved antenna panel includes redesigned L-band elements mounted on the SV's Earth-facing structure in the same way as the original 'legacy' antenna panel. This provided a stepping-stone toward the new modernized Block IIR-M SV launched in 2005 and has benefitted all GPS users with increased signal strength.

Following a discussion of background concepts, this paper presents the antenna performance requirements, highlights design features of both the legacy and improved antenna panels, and examines antenna panel performance. Finally, the antenna panel patterns of both antenna designs are also described as well as its use on orbit.

BACKGROUND

In 1989, Lockheed Martin Space Systems Company and its payload system subcontractor, Harris/Exelis/ITT were put on contract to build the GPS Block IIR SV (Figure 1). The direction to upgrade 8 of the original 21 SVs into the modernized Block IIR-M version was given in 2001. The exterior view of the IIR-M SV is very similar to the IIR SV (Figure 1), with the exception of the antenna panel.

Figure 1. Two Renderings of the GPS Block IIR SV

https://doi.org/10.33012/2016.14596

Between 1997 and 2009, 20 IIR/IIR-M SVs were placed on-orbit to form the largest portion of the GPS constellation. These SVs, as operated by the Second Space Operations Squadron (2 SOPS) of the Air Force Space Command (AFSPC), continue to provide exceptional accuracy and availability on-orbit [2][3]. The first of the original 21 IIR SVs, Space Vehicle Number 42 (SVN42), was destroyed in a booster accident [4]. The 8 final SVs were retrofitted to incorporate the improved antenna panel, modernized L-band boxes [5][6], and other improved components.

The GPS Block IIR and IIR-M SVs were built with one of two different antenna panel types. The original legacy antenna panel was used on the first 8 of 12 classic IIR SVs. The improved antenna panel was used on the final 4 of 12 classic IIR SVs, and on all 8 of the modernized IIR-M SVs. The GPS Block IIR improved antenna includes new antenna element designs and configurations on the panel, which will be described later in this paper. Table 1 shows which panel type was used on which SV version, with the SVs listed in launch order from first to last.

Table 1. IIR/IIR-M Versions

SVN (Launch Order)	SV Type		Antenna Panel Type	
	Classic IIR SV	IIR-M SV	Legacy Antenna Panel	Improved Antenna Panel
43	√		√	
46	√		√	
51	√		√	
44	√		√	
41	√		√	
54	√		√	
56	√		√	
45	√		√	
47	√			√
59	√			√
60	√			√
61	√			√
53		√		√
52		√		√
58		√		√
55		√		√
57		√		√
48		√		√
49		√		√
50		√		√

This table also indicates the 8 SVs which were updated from the classic IIR SV configuration to the modernized IIR-M configuration. All SVs with the improved antenna panel have increased power compared to the legacy panel. The 8 IIR-M SVs also provide additional power due to higher power transmitters. The new transmitters have the option to increase power in a few selected configurations. The total power envelope is further increased on IIR-M SVs with the new modernized signals.

ANTENNA PERFORMANCE REQUIREMENTS

The signal strength for L1 and L2 frequencies is specified by requirements, and was measured in factory test and in on-orbit operation with the specific criteria defined at edge of Earth (EoE). EoE is defined as 5° elevation to the ground-based terrestrial user. This is equivalent to 13.8° from antenna boresight for the Earth-facing (nadir) SV antenna panel. Both terrestrial service and space service requirements will be discussed in this section.

GPS Terrestrial Service Requirements

The IIR and IIR-M SV broadcast power requirement specifications, as well as factory and on-orbit measured performance data, are quantified in terms of L-band signals and code power at EoE [7]. This is the signal power as received by a terrestrial user. Table 2 shows the L-band power requirements for the various IIR SV configurations and signals. This table lists the IIR/IIR-M SV system-level specification requirements defined by the Air Force. The SV was built to meet these requirements. Also shown in the table are the 'derived' total power values for the L1 and L2 frequencies. For L2, this derived value is unchanged for the classic IIR SV since the only code that is carried by L2 is L2P. For L1, the derived total power value is the summation of the L1C/A and L1P values.

Table 2. IIR/IIR-M SV System Specification L-Band Power Requirements (dBW)

	IIR with Legacy Panel	IIR with Improved Panel	IIR-M	IS-GPS-200H Req [8]
L1 C/A	-160.0	-160.0	-158.7	-158.5
L1P	-163.0	-163.0	-160.6	-161.5
L1M	—	—	-158.0	-158.0*
L1 Total (Derived)	-158.2	-158.2	-154.2	-154.3
L2C	—	—	-161.4	-160.0**
L2P	-166.0	-166.0	-160.9	-161.5
L2M	—	—	-161.4	-161.0*
L2 Total (Derived)	-166.0	-166.0	-156.5	-156.5**

* Air Force specification

** Per LMSSC exception letter, L2C should be -161.4 dBW

The specified received signal strength for the IIR legacy panel (Table 2, column 2) is defined as the signal strength received by a +3 dBi linear antenna. This received strength is attenuated by a 0.5 dB atmospheric loss for the worst case link (minimum antenna gain and minimum transmitter power) and a 2.0 dB atmospheric loss for the nominal link (nominal gain and transmitter power). The IIR SV with the improved antenna panel was required to meet the same specifications (Table 2, column 3).

The received signal strength for IIR-M is defined in the revised Air Force specification as the signal strength received by a 0 dBi circularly polarized antenna with a 0.5 dB atmospheric loss for the worst case link (minimum antenna gain and minimum transmitter power, averaged about azimuth). The '0 dBi' power levels are specified as -157.7 dBW for L1 C/A, -159.6 dBW for L1P,

-157.0 dBW for L1M, -160.0 dBW for L2C, -159.6 dBW for L2P, and -160.0 dBW for L2M. In order to compare the IIR-M specifications with the IIR values, these circular 0 dBi values must be converted into the +3 dBi linear antenna values. This is accomplished by considering the antenna's axial ratio requirements and the resultant impact to the link. The revised IIR-M requirements, as received by a +3 dBi linear antenna, are roughly equal to the values recorded in Table 2, column 4.

Table 2, column 5 shows the GPS Interface Specification (IS) [8] performance expected by the user. The IS requirements provided guidance to the SV specifications. The IIR SV design requirements were originally based on an earlier version of the specifications. The most recent Revision H (as well as every version since revision D) specifies higher power and modernized requirements. The 1.5 dB change in the IS between the earlier version and Rev. H is due to the removal of conservatism in the atmospheric losses in the link budget. The table also shows the derived values for total power on L1 and L2.

This power is required to extend from nadir to EoE for the classic IIR and IIR-M SVs (13.8° half-cone; a 27.6° cone). This terrestrial service volume is defined as the near-Earth region up to 3,000 km altitude (see Figure 2).

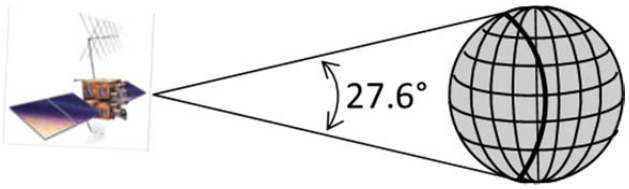

Figure 2. Earth Terrestrial Service Volume Definition

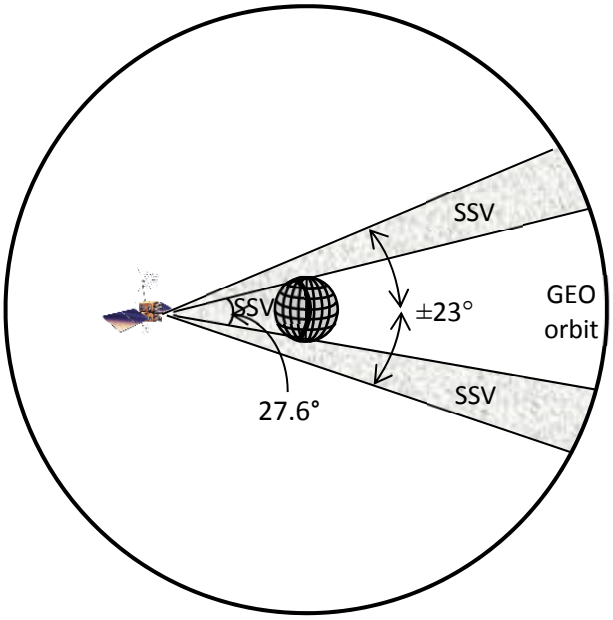

Figure 3. Space Service Volume Definition

GPS Space Service Requirements

For GPS Block IIF SVs, the broadcast signal also has an orbital environment requirement to extend out from EoE to 23° off-nadir. This is called the space service volume (SSV) (Figure 3) [9][10]. The SSV is defined as the spherical shell up to 36,000 km altitude (approximately the geosynchronous orbit altitude). The new GPS III SV also has an SSV requirement which is defined at 23.5° for L1 and 26° for L2 and L5.

Table 3 summarizes the SSV requirements for GPS Block IIF and GPS III. The SSV is not a requirement for GPS Block IIR/IIR-M SVs, but some service is available. This will be discussed later in the paper.

Table 3. GPS Block IIF and GPS III Space Service Volume Requirements

	GPS Block IIF*		GPS III*	
	from EoE out to 20° off-nadir	from EoE out to 23° off-nadir, decrease monotonically down to …	from EoE out to 23.5° off-nadir	from EoE out to 26° off-nadir, decrease monotonically down to …
L1 C/A (dBW)	< 10 dB decrease	< 18 dB decrease	-184.0	N/A
L1 P(Y) (dBW)			-187.0	
L2 P(Y) (dBW)	N/A	< 10 dB decrease	N/A	-186.0
L2C (dBW)				-183.0

*Ref. IS-GPS-200H [8]

GPS IIR/IIR-M ANTENNA PANEL DESCRIPTION

The two antenna panel variations are the legacy antenna panel and the improved antenna panel. This section will highlight some of the basic design features of each, with an emphasis on the differences.

Legacy Antenna Panel Design

The GPS Block IIR legacy antenna panel is pictured in Figure 4 (left side). This panel was installed on the first 8 of 12 IIR SVs. It consists of 8 helix elements positioned in a circle with 4 helix elements in the center on the Earth-facing antenna panel. These elements are the taller, thinner, pointed structures seen in the picture. The shorter,

thicker, antenna elements seen in Figure 4 serve the ultra-high frequency (UHF) communications of the SV. This subsystem is beyond the scope of this paper.

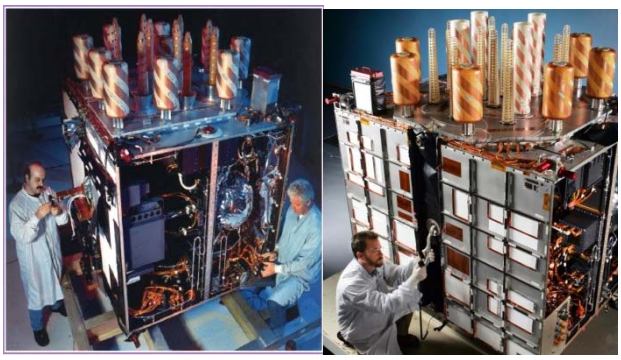

Figure 4. Legacy (Classic) and Improved Antenna Panels

The 12 antenna elements are fed by a low loss Beam Forming Network (BFN) consisting of several coaxial cables and a 12-way power divider. The BFN supplies a weighted signal power distribution to the elements, including the addition of a phase offset between the two rings. This differential phasing provides a balanced power over the horizon-to-nadir Earth coverage range of the antenna panel (13.8°).

The nominal antenna panel directivity pattern curves from the two rings are shown in Figure 5. The directivity pattern from the inner ring of 4 L-band elements (a wide-angle broadcast) combined with a phase-offset of the directivity pattern from the outer 8 L-band elements (a narrow-angle broadcast) produces a total pattern with the desired Earth-shaped result. Overall, the array forms a shaped, 27.6° Earth coverage pattern with signal power roll-off and sidelobes extending beyond the EoE.

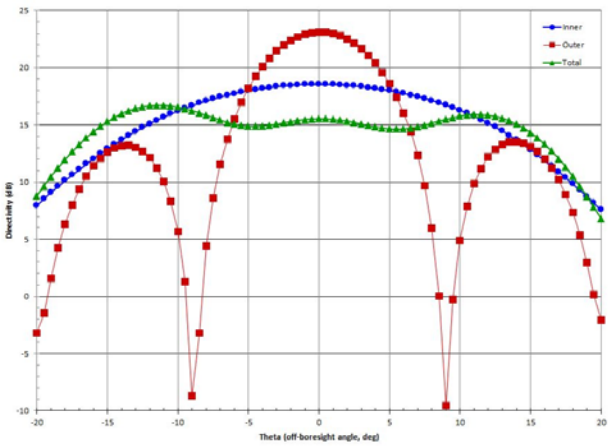

Figure 5. Nominal Antenna Panel Pattern from Inner and Outer Rings

Improved Antenna Panel Design

The final 4 classic IIR and all 8 modernized IIR-M SVs were retrofitted with the improved antenna panel [11]. This panel is pictured in Figure 4 (right side). The new panel reused the existing structure and L-band transmitter interface. New element designs and optimized alignment on the panel provide the improved performance.

The new L-band elements are formed from copper wire in a helix shape on a tapered G10 core as opposed to the earlier design of copper tape on a cylindrical structure with a conical top.

As with the legacy panel, a BFN distributes the L-band power to the antenna elements. This provides the proper amplitude weighting and phasing between the inner and outer rings.

Antenna Panel Coordinate System and SV Mounting Alignment

This section describes the antenna panel coordinate system and the mounting alignment (orientation) of the antenna panel on the SV. This information may be used in conjunction with the IIR SV yaw model [12][13] as will be discussed later in this paper and can be used to predict the alignment of the broadcast L-band pattern at a particular receiver location, as is done in reference [14].

The IIR SV body axes are shown in Figure 6. They are defined as:

- +Z axis directed toward Earth (nadir)
- +Y axis along the 'positive' solar array axis
- +X completes right-handed system

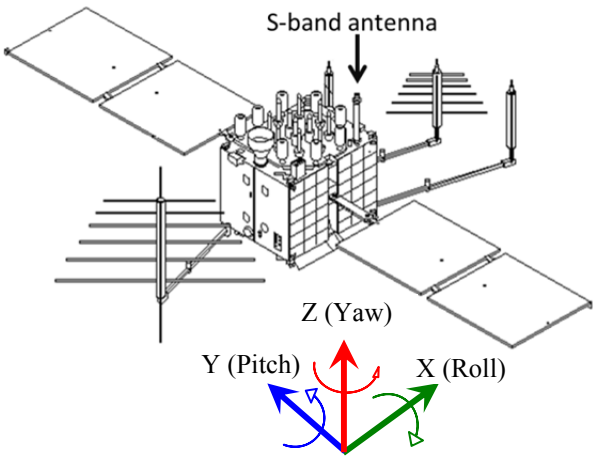

Figure 6. SV Body Axis Definition

The location of the S-band antenna is identified in Figure 6 to serve as a reference point. The antenna panel is oriented on the SV such that the tall S-band antenna element is located in the (+X, -Y) corner of the SV

structure. Both versions of the antenna panels are mounted to the SV structure in the same orientation.

Antenna Panel Pattern Measurement Coordinates

The antenna panel pattern measurement coordinates are defined by two angles: phi (φ) and theta (θ). The angles φ and θ are used in the description of the antenna panel patterns later in this paper. Refer to Figure 7 and Figure 8 for visualization of the φ and θ angle definitions. The view of the SV in Figure 7 is in the –Z direction (into the antenna panel).

- φ = the angle that is counter-clockwise around the antenna panel boresight (earth-facing) axis with a range of 0° - 360° (Figure 7). The axis of rotation of φ is around the SV +Z axis (which is in the direction of the SV yaw attitude angle), with φ = 0° referenced to the IIR SV +X axis.
- θ = the angle that is across the face of antenna panel, from the +Y solar array (θ = -90°), through the nadir direction (θ = 0°), to the -Y solar array (θ = +90°) (Figure 8). The axis of rotation of θ is around the SV +X axis. Recall that the EoE boresight angle is defined as θ = ±13.8° for the GPS orbit.

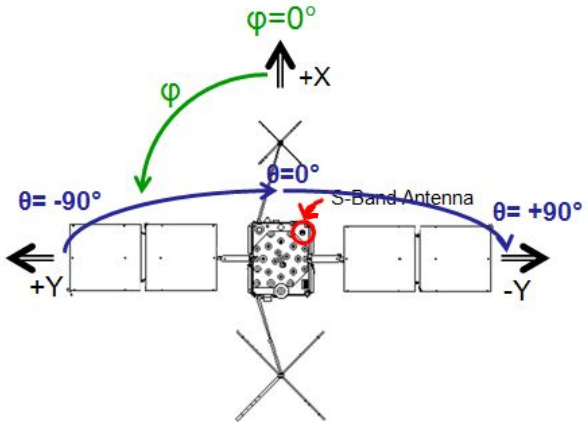

Figure 7. Antenna Orientation Angles: Around Boresight (phi, φ) and Off-Boresight (theta, θ)

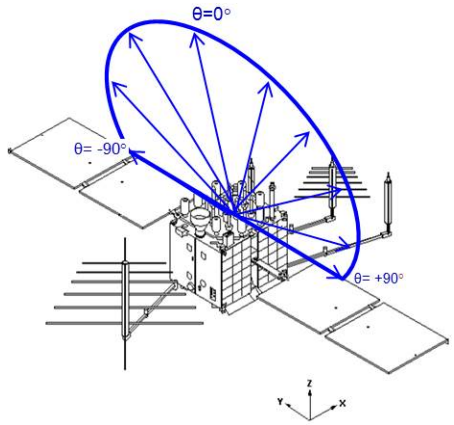

Figure 8. Antenna Orientation - Off-Boresight, Side View

The antenna panel mounting orientation on the Earth face of the IIR SV is specified as having the panel reference line, φ = -90°, aligned along the -Y SV body axis (SV S-band antenna boom in the 'upper right' corner). This can be seen in Figure 7.

IIR YAW ATTITUDE

The nominal operational 3-axis stabilized flight attitude for the GPS Block IIR/IIR-M SV is called Sun-Nadir Pointing (SNP). This mode uses the Earth and Sun sensors to maintain the SV's X-Z plane to be in the Sun-Vehicle-Earth (SVE) plane with the SV yaw axis (+Z) aligned with nadir (toward Earth center, see Figure 9). This keeps the pitch (Y) axis normal to the SVE plane as the solar arrays are pointed at the sun.

Note, that in SNP, the -X face generally points toward the sun in order to provide better thermal management of the payload on the +X side of the SV.

The yaw attitude is defined as the angle from the orbit velocity vector to the vehicle's +X axis. Figure 6 showed the roll, pitch, and yaw angles around the +X, +Y, and +Z axes, respectively. Figure 9 shows the notional SNP orbit, including:

- Alpha angle (α) defined as the orbit plane angle from the point closest to the Sun ('orbit noon') to the SV (range of 0 – 360 deg).
- Beta angle (β) defined as the angle from the orbit plane to the sun plane (above or below, nominally ± 79 deg).
- The orbit 'cardinal points' of:
  - orbit noon (α=0º)
  - orbit dusk (α=90º)
  - orbit midnight (α=180º)
  - orbit dawn (α=270º)

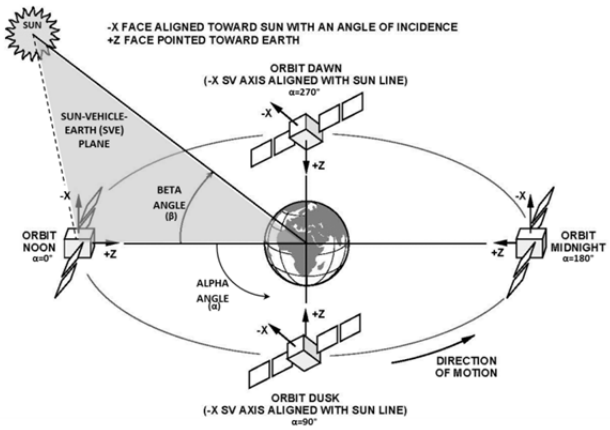

Figure 9. GPS SNP Orbit Geometry

The yaw angle and yaw rate are presented in equations (1) and (2).

$$\text{Yaw Angle} = \arctan\left(\frac{\sin\beta}{\sin\alpha * \cos\beta}\right) \quad (1)$$

$$\text{Yaw Rate} = -n * \left(\frac{\cos\alpha * \tan\beta}{\sin^2\alpha + \tan^2\beta}\right) \quad (2)$$

Where n is the mean motion of the orbit (mean orbit rate):

$$n \equiv \sqrt{\frac{\mu}{a^3}} \quad (3)$$

with:
μ = the earth gravitational parameter (3.986005E14 m3/sec2 (WGS 1984))

a = the mean semi-major axis of the SV orbit

As the beta angle approaches 0 deg, noon and midnight turns of as much as 180 deg are performed to maintain the SNP attitude. The solar arrays are commanded perpendicular to the sun line as computed on-board based on the SV α and β angles. Roll, pitch, and yaw attitude rates are commanded to maintain the SNP attitude. The Yaw Rate is limited to 0.20 deg/sec.

Figure 10 and Figure 11 illustrate the SNP yaw angles for positive and negative Beta values relative to where the SV is in its orbit position (alpha angle).

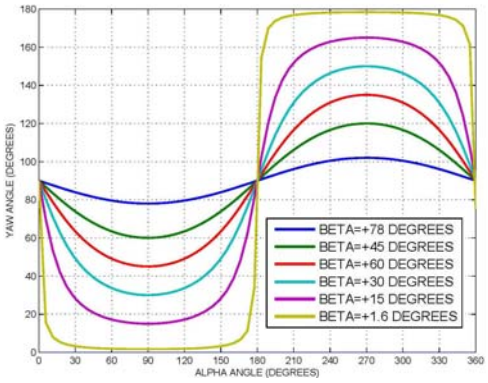

Figure 10. SNP Yaw Angle vs. Orbit Alpha, for Positive Beta Values

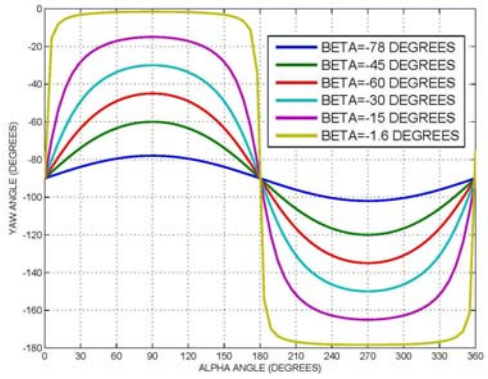

Figure 11. SNP Yaw Angle vs. Orbit Alpha, for Negative Beta Values

THE GPS IIR/IIR-M ANTENNA PANEL PERFORMANCE

This section will present the factory and on-orbit performance measurements for the L1 and L2 signals on both the legacy and improved antenna panels. The focus will be on the signal strength received by the terrestrial user and its comparison with the specifications described earlier in the paper.

The GPS signal, on each of the L1 and L2 frequencies, is spread through the application of a pseudo-random noise (PRN) code sequence [15]. The classic IIR SVs, with either antenna panel version, have only one code sequence, the precision code (P-code), applied to L2 (thus, abbreviated as 'L2P'). On the L1 frequency, there are two different code sequences, C/A and P (thus, 'L1C/A' and 'L1P', respectively).

On the newer IIR-M SVs, L1 still has the same two original code sequences as the IIR SVs (L1C/A and L1P), but L2 has a second code sequence, L2C. In addition, both L1 and L2 have side-lobes from a binary offset carrier (BOC) that host the new military code (M-code) sequence (L1M and L2M). These new, modernized code sequences and BOC sidelobes increase the total broadcast signal power envelope.

The varying code sequence combinations on the broadcast frequencies affect the signal performance analysis. Comparisons of received signal strength should only be made in terms of code power levels. Combined signal power is generally only applicable to SV system considerations. For example, classic IIR L2P should only be compared to IIR-M L2P, excluding L2C and L2M.

On-Orbit Code Power Performance

This section will examine the code power results for both L1 and L2, as opposed to the total power measurements seen in the previous three sections. For L1, the code power comparison is shown for several SVs in Figure 12: SVN30 (a Block IIA), SVN51 (a Block IIR with a legacy antenna panel), SVN47 (a Block IIR with an improved antenna panel), and SVN53 (a Block IIR-M).

The plot shows three groups of curves, distinguishing the several code power levels. The lowest grouping shows L1P power for SVNs 30, 51, 47, and 53, in ascending order based on the EoE values. The middle grouping in Figure 12 shows L1 total power (L1C/A plus L1P) for SVNs 30, 51, and 47 in ascending order. The top line in the plot shows the SVN53 total power (L1C/A plus L1P plus L1M). Also shown in the figure are the specification requirements to be met at EoE for each of the codes. It can be seen that all SVs exceed the specified

requirements. To avoid unnecessary plot complexity, L1C/A is not shown.

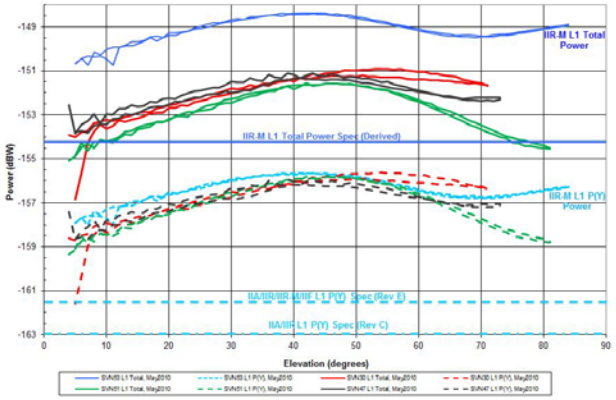

Figure 12. Code Power Measurements - L1

The L1M and L2M specific power levels have been previously reported [1] and found to exceed specified required levels at all points.

In a similar fashion, Figure 13 shows three code power groupings for L2: L2P, L2C, and L2 total. The specification requirements are also shown. This figure shows that all SVs exceed the specified requirements.

Reference [1] presented factory measured performance as well as other on-orbit performance plots and analysis.

Summation of Performance Results, Terrestrial and Space

Table 4 shows a comparison between the requirements and the performance of the classic IIR SVs with the improved antenna panel. The IIR legacy panel exceeds specifications for L1 (L1P and L1C/A), and for L2 (L2P). The improved panel on the classic IIR SVs (with a higher specification level) exceeds specifications for L1 (L1P and L1C/A) and for L2 (L2P). The improved panel on the IIR-Ms SV (also with a higher specification level) exceeds specifications for L1 (L1P, L1C/A, and L1M) and for L2 (L2P, L2C, and L2M).

The results show that IIR performance exceeds all IS requirements, and the IIR improved antenna panel provides a stronger terrestrial service signal. The new IIR-M SV also performs better, due to the higher power L-band transmitters combined with the improved antenna panel.

Table 5 shows SSV results for both the legacy and improved panels. The results show that some SSV is available from IIR and IIR-M, though not all levels specified for GPS Block IIF and GPS III are met. Recall that the SSV service is not a requirement for GPS Block IIR/IIR-M. The IIR improved panel provides stronger SSV signal than the legacy panel.

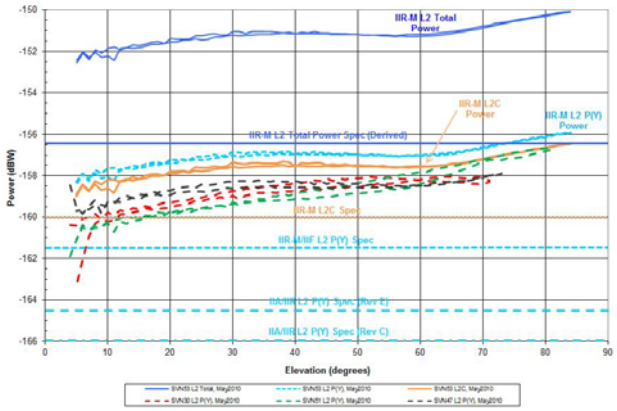

Figure 13. Code Power Measurements - L2

THE GPS IIR/IIR-M ANTENNA PANEL PATTERN

The antenna panel pattern is recorded and presented in terms of beam directivity and phase across the face of the panel. Directivity is the signal power density in a specific direction. Average directivity plots are presented later in this paper for both antenna panel types. SV-specific pattern plots and data, including the directivity, are available online.[1]

The antenna panel pattern is described by beam directivity and phase around the shape of the panel in θ and φ coordinates. The plots presented in this section are the average directivity for each type of antenna panel at the L1 and L2 frequencies. SV-specific plots and data for the 20 GPS Block IIR/IIR-M SVs are available online. The directivity measurement uncertainty is typically +/-0.25 dB.

Antenna gain (G) is derived from the directivity (D) by applying the gain correction factor (GCF) value for each SV using equation (4).

$$G = D + GCF \qquad (4)$$

The gain correction factor, GCF, is computed from the measurement of a standard gain horn, the measurement of the panel, and the directivities for each frequency. It is the antenna loss in dB at the L1 and L2 frequencies. Table 6 provides the measured GCF values at L1 and L2 for all IIR and IIR-M SVs.

[1]SV-specific directivity plots, as well as SV-specific directivity and phase data, are available online at http://www.lockheedmartin.com/us/products/gps/gps-publications.html.

Table 4. Legacy and Improved Panel Results vs. Terrestrial Requirements (dBW)

	IIR System Requirements IIR/IIR-M	IS Rev H Requirements [8] IIR/IIR-M	Classic IIR SV Legacy Panel Measured Performance	Classic IIR SV Improved Panel Measured Performance	IIR-M SV Improved Panel Measured Performance
L1 C/A	-160.0/-158.7	-158.5	-157.7	-156.9	-155.2
L1P	-163.0/-160.6	-161.5	-159.2	-158.7	-157.9
L2C	—/-161.4	—/-160.0*	—	—	-158.9
L2P	-166.0/-160.9	-164.5/-161.5	-161.8	-159.4	-158.4

* Per LMSSC exception letter, L2C should be -161.4 dBW

Table 5. IIR/IIR-M Space Service Volume Results

	Though not a IIR requirement, the following service is provided at the levels presented in IS-GPS-200H:			
	L1, at 20° off-nadir	L1, at 23° off-nadir	L2, at 23° off-nadir	L2, at 26° off-nadir
IIR Legacy Panel	At some SV yaw angles	At some SV yaw angles	Yes	At some SV yaw angles
IIR Improved Panel	At some SV yaw angles	Yes	Yes	Yes

Table 6. IIR/IIR-M Gain Correction Factor (GCF) Values

SVN (Launch Order)	L1 GCF (dB)	L2 GCF (dB)
43	-0.9	-1.1
46	-1.0	-1.2
51	-0.7	-1.2
44	-1.1	-1.0
41	-0.9	-1.1
54	-0.8	-1.0
56	-0.7	-1.1
45	-1.1	-1.2
47	-1.3	-0.8
59	-1.3	-0.8
60	-1.3	-0.7
61	-1.2	-0.8
53	-1.4	-0.8
52	-1.2	-0.7
58	-1.3	-0.9
55	-1.3	-0.8
57	-1.3	-0.8
48	-1.4	-0.9
49	-1.3	-0.8
50	-1.3	-0.8

Average Antenna Panel Pattern - L1 Signal

The average L1 directivity pattern from both the 8 legacy and 12 improved panels will be presented and compared in this section. SV-specific plots and data for the 20 GPS Block IIR/IIR-M SVs are available.

Legacy Antenna Panel Pattern, L1 Signal

The legacy antenna pattern for L1 is seen in Figure 14. This figure shows plots of the average of the 8 legacy panels for L1 directivity as a function of off-boresight angle (θ), for φ cuts every 10°. Each of the 36 curves (in φ) in the complex plot is a cut through the broadcast pattern with θ varying from -90° to +90°. The terrestrial service is labeled ('Earth Service') on the plot for θ = -13.8° to θ = +13.8°. The space service is from θ = -13.8° to θ = -90° (the left side of the plots) as well as from θ = +13.8° to θ = +90° (the right side of the plots). These plot ranges cover well beyond the specific SSV definition in Figure 3.

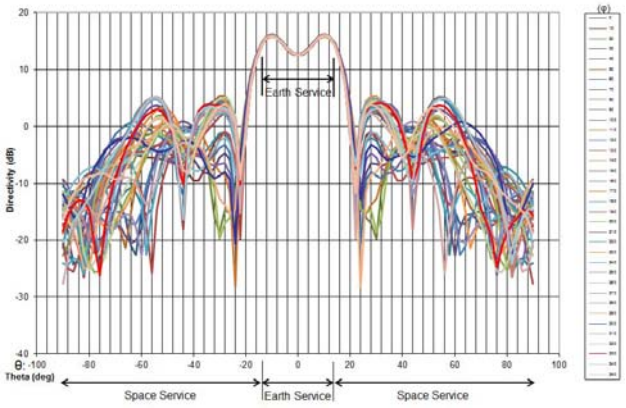

Figure 14. Average Legacy Antenna Pattern - L1

The Earth-shaped pattern is clearly seen for the designated Earth service region. At the edge of each side of the Earth service pattern, the directivity drops off significantly to the -20° or +20° angle off-boresight. Beyond that, on each side of the plot, the side-lobes of the signal are seen to vary significantly over the changing φ angle.

Improved Antenna Panel Pattern, L1 Signal

The improved antenna pattern is seen in Figure 15 and Figure 16. This figure shows plots of the average of the

12 improved panels for L1 directivity as a function of off-boresight angle (θ), for φ cuts every 10°.

Table 7 presents a comparison between the legacy and the improved antenna panels for the L1 directivity pattern. The terrestrial service is indicated by the EoE performance and the SSV service is indicated by the signal beyond EoE.

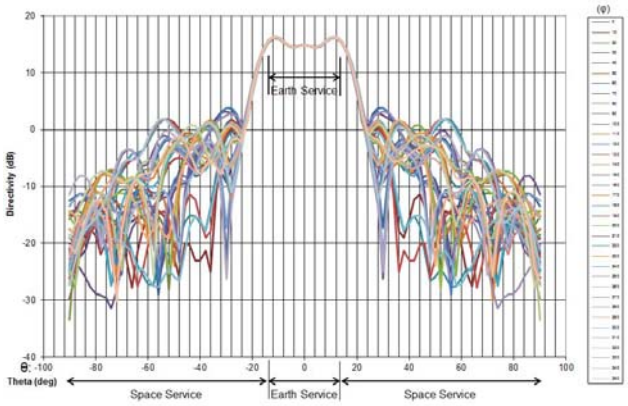

Figure 15. Average Improved Antenna Pattern - L1

It is observed that at EoE, the improved panel signal strength is +1 dB over the legacy panel.

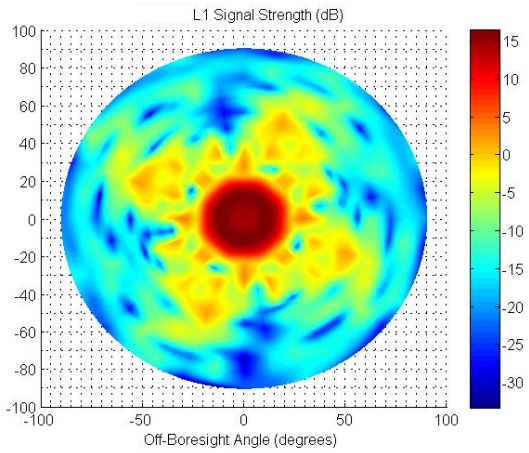

Figure 16. Average Improved Antenna Pattern - L1, 3-D Plot

Average Antenna Panel Pattern - L2 Signal

The average L2 directivity pattern from both the legacy and improved panel will be presented and compared in this section.

Table 7. Legacy vs. Improved Panel - L1

	Edge of Earth (EoE) (dB)	EoE out to 20°		EoE out to 23°	
		Magnitude (dB)	Reduction (dB)	Magnitude (dB)	Reduction (dB)
Legacy Panel	+15	+4 to -5	-11 to -20	-2 to -19	-17 to -34
Improved Panel	+16	+9 to +5	-7 to -11	+2 to -4	-14 to -20
Change from Legacy to Improved	+1	+5 to +10		+4 to +15	

Legacy Antenna Panel Pattern, L2 Signal

The legacy antenna pattern is seen in Figure 17. This figure shows plots of the average of the 8 legacy panels for L2 directivity as a function of off-boresight angle (θ), for φ cuts every 10°.

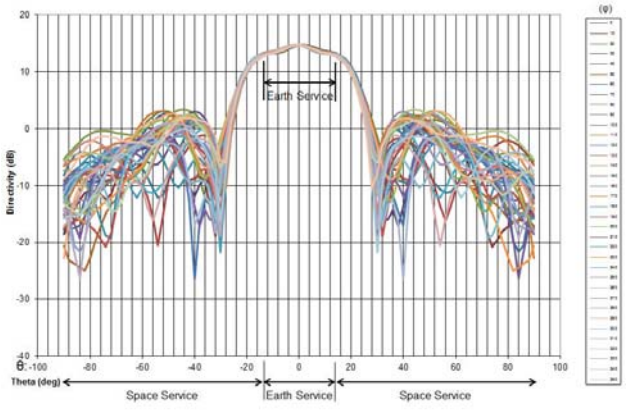

Figure 17. Average Legacy Antenna Pattern - L2

Improved Antenna Panel Pattern, L2 Signal

The improved antenna pattern is seen in Figure 18. This figure shows plots of the average of the 12 improved panels for L2 directivity as a function of off-boresight angle (θ), for φ cuts every 10°.

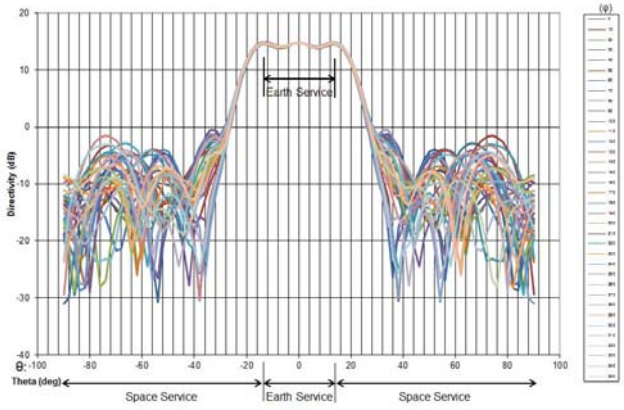

Figure 18. Average Improved Antenna Pattern - L2

Table 9 presents a comparison between the legacy and the improved antenna panels for the L2 directivity pattern. The terrestrial service is indicated by the EoE performance and the SSV service is indicated by the signal beyond EoE.

It is observed that at EoE, the improved panel signal strength is +2 dB over the legacy panel.

SV ANTENNA PHASE CENTER

The L-band signal antenna phase center is a measurement of the offset of the broadcast signal phase center relative to the SV's center of mass. It is measured at the factory.

Table 8 presents a recent set of SV antenna offset values relative to the SV body centered coordinates in meters [16].

Table 8. IIR/IIR-M Antenna Phase Center Values (m)

Block Type	PRN	Delta-X	Delta-Y	Delta-Z
II/IIA	ALL	0.2794	0.0000	0.9519
IIR	02	-0.0099	0.0061	-0.082
IIR	11	0.0019	0.0011	1.5141
IIR	13	0.0024	0.0025	1.614
IIR	14	0.0018	0.0002	1.6137
IIR	16	-0.0098	0.006	1.663
IIR	18	-0.0098	0.006	1.5923
IIR	19	-0.0079	0.0046	-0.018
IIR	20	0.0022	0.0014	1.614
IIR	21	0.0023	-0.0006	1.584
IIR	22	0.0018	-0.0009	0.0598
IIR	23	-0.0088	0.0035	0.0004
IIR	28	0.0019	0.0007	1.5131
IIR-M	05	0.00292	-0.00005	-0.01671
IIR-M	07	0.00127	0.00025	0.00056
IIR-M	12	-0.01016	0.00587	-0.09355
IIR-M	15	-0.00996	0.00579	-0.01227
IIR-M	17	-0.00996	0.00599	-0.1006
IIR-M	29	-0.01012	0.00591	-0.01512
IIR-M	04	0.01245	-0.00038	-0.02283
IIR-M	31	0.0016	0.00033	-0.0575
IIF	01	0.391	0.0000	1.091
IIF	03	0.395	0.0003	1.0907
IIF	06	0.3947	-0.001	1.0917
IIF	08	0.3962	-0.0003	1.0856
IIF	09	0.3955	-0.002	1.0922
IIF	10	0.3962	-0.0013	1.0831
IIF	24	0.392	0.002	1.093
IIF	25	0.392	0.002	1.093
IIF	26	0.3934	-0.0011	1.0927
IIF	27	0.3914	0.0003	1.0904
IIF	30	0.3952	-0.0008	1.0904
IIF	32	0.3966	-0.0002	1.0843

Table 9. Legacy vs. Improved Panel - L2

	Edge of Earth (EoE) (dB)	EoE out to 23°		EoE out to 26°	
		Magnitude (dB)	Reduction (dB)	Magnitude (dB)	Reduction (dB)
Legacy Panel	+13	+9 to +5	-5 to -9	+5 to -3	-9 to -17
Improved Panel	+15	+9 to +6	-6 to -9	+5 to 0	-10 to -15
Change from Legacy to Improved	+2	0 to +1		0 to +3	

SV GROUP DELAY

The L-band signal group delay value (TGD or T_{GD}) for the L1-to-L2 signal correction on each SV is initially measured at the factory. With the advent of the modernized signals, this is more generally called the inter-signal correction (ISC) [17] and is computed for each unique pair of signals relative to L1.

Following placement on-orbit, it has been determined by 2 SOPS that better accuracy of this T_{GD} measurement is obtained through estimation of these parameters by the Jet Propulsion Laboratory (JPL). Every quarter, these values are estimated and delivered to 2 SOPS after which updated values are entered into the database and broadcast in the navigation message (subframe 1, word 7, see [8]). Table 10 presents a recent set of T_{GD} values.

Table 10. IIR/IIR-M TGD Values

PRN	SVN	Broadcast Tgd (ns)
1	63	5.12
2	61	-20.49
3	69	1.40
4	49	-19.56
5	50	-10.71
6	67	4.19
7	48	-11.17
8	72	5.12
9	68	1.40
10	73	2.33
11	46	-12.11
12	58	-12.57
13	43	-11.17
14	41	-9.31
15	55	-10.71
16	56	-10.71
17	53	-10.71
18	54	-11.17
19	59	-14.90
20	51	-8.38
21	45	-9.78
22	47	-17.69
23	60	-20.02
24	65	2.33
25	62	5.59
26	71	6.98
27	66	1.86
28	44	-10.71
29	57	-10.24
30	64	3.72
31	52	-13.50
32	70	0.93

IIR ANTENNA PATTERN USE IN ORBIT

The GPS Block IIR/IIR-M signals are currently being used or studied for use by many on-orbit, or planned, missions. Recent SSV use of the GPS signal is reflected in references relating to geosynchronous use such as [18], [19], [20], [21] [22], [23], [24], [25], [26], [27], [28], [29], [30], [31] and [32], references relating to high Earth orbit use such as [33], [34], [35], and [36], and references relating to use for Lunar missions, such as [37], [38], and [39]. A few of these will be discussed further.

The Antenna Characterization Experiment (ACE) mission is hosted on a geosynchronous platform and has collected extensive measurements of the GPS L1 signal from all available SVs [18]. The data collected by ACE are the first in-flight measurements of the GPS IIR antenna pattern, in particular, the beam side lobes. This performance analysis generally aids high-altitude satellite navigation and mission planning.

Figure 19 shows the reconstructed antenna panel pattern for the GPS Block IIR/IIR-M improved antenna panel. It compares exceptionally well with the pattern seen in Figure 16.

Another interesting use of the extended antenna signal on-orbit is the Magnetospheric MultiScale (MMS) mission. MMS employs four identical spacecraft flying a close formation in a highly eccentric orbit to investigate the Earth's dayside magnetopause and the night-side neutral sheet [40]. Figure 20 shows the MMS tracking of GPS SVs over a several-day period last year.

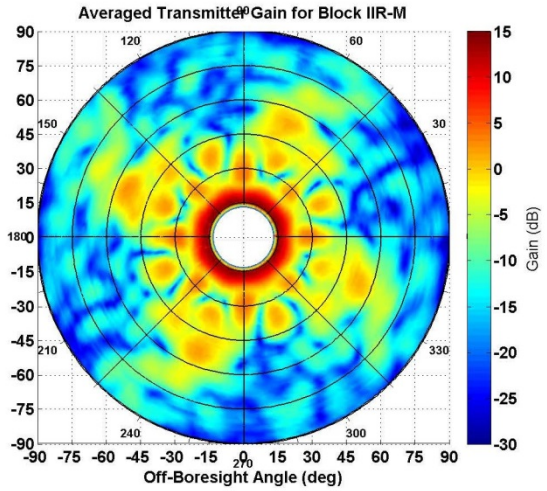

Figure 19. ACE Measurement of the Average GPS Block IIR-M Antenna Signal [18]

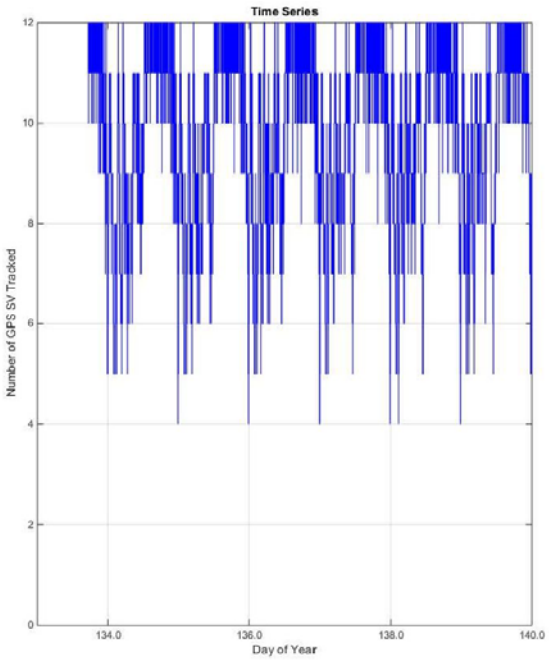

Figure 20. GPS SV Tracking by the Magnetospheric MultiScale Satellites [40]

The number of GPS SVs tracked by MMS decreases as expected at the very high apogee altitude (above 10 R_{EARTH}), but proved to exceed pre-launch expectations in both number and duration. The specific GPS Block IIR/IIR-M antenna panel patterns presented in this paper and its preceding reference [1] were used in MMS navigation performance analysis [40][41].

Similarly, NASA has used and is using these antenna panel patterns in a number of other programs:

- Geostationary Operational Environmental Satellite R-series (GOES-R) [42]
- Cyclone Global Navigation Satellite System (CYGNSS) [31]
- Global Precipitation Measurement (GPM)
- Neutron-star Interior Composition Explorer (NICER)
- Global Ecosystem Dynamics Investigation (GEDI)
- Dellingr
- Several high-altitude CubeSat concepts

This includes maximizing the use of the GPS sidelobes which have previously been poorly known [41].

The European Space Agency (ESA) has used this pattern data in validation of their space environment simulators. This was done primarily in support of GPS signal use for a Lunar mission [40][43][44].

The German Aerospace Center (Deutsches Zentrum für Luft- und Raumfahrt; DLR) has used these patterns to assist in tracking the performance of the on-orbit GPS Block IIR/IIR-M SVs. Current work involves using the patterns to support the analysis of relative navigation in highly eccentric orbits [45].

Measurement of the antenna pattern (Figure 21) for every GPS SV is being done from a single site (Palo Alto/Menlo Park, CA) [46]. This is performed on a regular basis (as often as monthly), to examine the status and trending of SV broadcast signal health and for potentially assisting during anomaly resolution. Over time, the SV attitude and orbit changes, as viewed from this single site. This data collection of these cross section patterns offers the opportunity to form a complete map of the actual antenna pattern for the each SV [14].

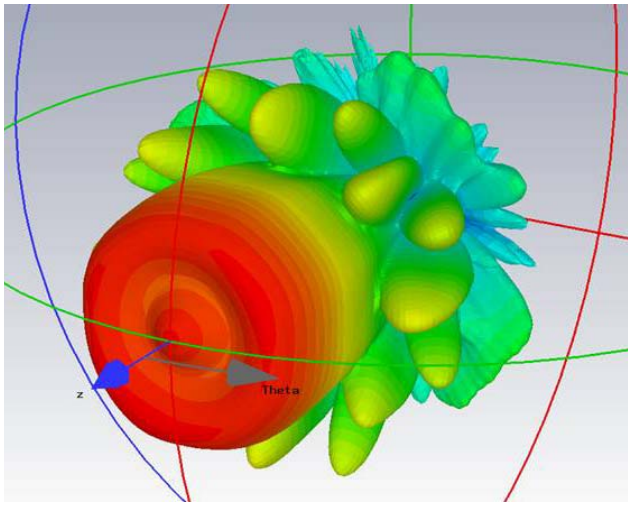

Figure 21. Notional GPS Signal Transmit Pattern with Sidelobes (from [42])

In addition to specific space mission support, the release of these patterns is encouraging the release of similar data from other GNSS systems, including signal sidelobes [47]. It also supports the formation of international SSV agreements in order to build an interoperable GNSS SSV. Finally, this antenna panel pattern information is being used to improve the products of the International GPS service (IGS) [45].

FUTURE WORK

With 20 GPS Block IIR/IIR-M SVs currently serving as the backbone of the GPS constellation, it is expected that they will continue to provide a quality broadcast L-band service for many years to come. These SVs will continue to be monitored regularly, as they remain active in the GPS constellation.

Additional ground testing of a spare or engineering design model of the improved antenna panel is being considered. This would be performd in a current test facility in order to validate and calibrate on-orbit measurements.

CONCLUSION

Presented in this paper are the GPS Block IIR/IIR-M antenna panel patterns. This information is of significant interest to SV designers and mission planners who use the GPS signal in terrestrial or space applications.

The results presented show that the GPS Block IIR and IIR-M SVs exceed all terrestrial service requirements for the GPS broadcast L-band power. The GPS Block IIR and IIR-M SVs provide much of the desired space service volume levels, though these are not applicable requirements to IIR. The GPS IIR improved antenna panel provides stronger terrestrial and space service.

Publishing this antenna panel data makes it publicly available for users around the world, enabling improved accuracy. This also sets a pattern for other GNSS systems to do the same.

ACKNOWLEDGEMENTS

The GPS Block IIR improved antenna panel development was funded under Lockheed Martin internal development funds and performed primarily at the LMSSC Communications and Power Center in Newtown, PA with support from subsystems specialists at the LMSSC Valley Forge IIR factory.

REFERENCES

[1] Marquis, W. and Reigh, D., "The GPS Block IIR and IIR-M Broadcast L-Band Antenna Panel - Its Pattern and Performance, NAVIGATION, Winter2015, DOI 10.1002, navi.123.

[2] Marquis, W., "Increased Navigation Performance from GPS Block IIR," *Navigation: Journal of the Institute of Navigation*, Vol. 50, No. 4, Winter 2003-2004, pp. 219-233.

[3] Marquis, W., "Recent Developments in GPS Performance and Operations," *Advances in the Astronautical Sciences, Guidance and Control 2011*, Vol. 141, Feb. 2011, pp. 3-21.

[4] Covault, C., "Delta Explosion Halts $1 Billion in Launches," *Aviation Week and Space Technology*, Vol. 146, No. 4, 27 Jan. 1997, pp. 30-33.

[5] Hartman, T., Boyd, L., Koster, D., Rajan, J., and Harvey, J., "Modernizing the GPS Block IIR Spacecraft," *Proceedings of the Institute of Navigation GPS 2000 Conference*, Sept. 2000, pp. 2115-2121.

[6] Marquis, W., "M is for Modernization: Block IIR-M Satellites Improve on a Classic," *GPS World*, Vol. 12, No. 9, Sept. 2001, pp. 38-44.

[7] Kaplan, E. and Hegarty, C., (ed.), *Understanding GPS: Principles and Applications*, 2nd ed., Artech House Publishers, Boston, 2006, Sect. 4.3.2.

[8] *NAVSTAR GPS Space Segment/Navigation User Interfaces*, IS-GPS-200H, GPS Directorate, Sep. 2013.

[9] Bauer, F., et al, "The GPS Space Service Volume," *Proceedings of the Institute of Navigation GNSS 2006 Conference*, Sept. 1995, Sept. 2006, pp. 2503-2514.

[10] Force, D., "Navigation Performance of Global Navigation Satellite Systems in the Space Service Volume," *Proceedings of the Institute of Navigation GNSS 2013 Conference, Sept. 2013.*

[11] Marquis, W. and Reigh, D., "On-Orbit Performance of the Improved GPS Block IIR Antenna Panel," *Proceedings of the Institute of Navigation GNSS 2005 Conference*, Sept. 2005, pp. 2418-2426.

[12] Bar-Sever, Y., "Performance Evaluation of the GPS Yaw Bias Implementation," *Proceedings of the Institute of Navigation GPS 1995 Conference*, Sept. 1995, pp. 599-611.

[13] Kouba, J., "A Simplified Yaw-attitude Model for Eclipsing GPS Satellites," *GPS Solutions*, Vol. 13, No. 1, Jan. 2009, pp. 1-12.

[14] Tetewsky, A., Okerson, G., et al, "White Paper for Establishing a Theoretical and Practical Process for Measuring and Reporting Min and Max Powers per ICD 200F, 705B, 700B, and 700A NATO with SVN45 as a Case Example," unpublished work, 2012.

[15] Kaplan, E. and Hegarty, C., (ed.), *Understanding GPS: Principles and Applications*, 2nd ed., Artech House Publishers, Boston, 2006, Sect. 4.2.1.

[16] http://earth-info.nga.mil/GandG/sathtml/gpsdoc2015_04a.html

[17] Tetewsky, A., Okerson, G., Ross, J., "Inter Signal Correction Sensitivity Analysis: Assessing SV Aperture Dependent Delays and Ground Control Approximations on Modernized GPS Dual Frequency Navigation," Institute of Navigation Joint Navigation Conference, June 2014.

[18] Martzen, P., Highsmith, D., Valdez, J., Parker, J., Moreau, M., "GPS Antenna Characterization Experiment (ACE): Receiver Design and Initial Results," Institute of Navigation Joint Navigation Conference, June 2015.

[19] Wu, S., Yunck, T., Lichten, S., Haines, B., Malla, R., "GPS-Based Precision Tracking of Earth Satellites from Very Low to Geosynchronous Orbits," *Proceedings of the National Telesystems Conference*, May 1992, pp. 4/1-4/8.

[20] Chao, C., and Bernstein, H., "Onboard Stationkeeping of Geosynchronous Satellites Using a Global Positioning System Receiver," *Journal of Guidance, Control, and Dynamics*, Vol. 17, No. 4, Jul. 1994, pp. 778-786.

[21] Ferrage, P., et al, "GPS Techniques for Navigation of Geostationary Satellites," *Proceedings of the 8th International Technical Meeting of the Satellite Division of the Institute of Navigation*, Sept. 1995, pp. 257-268.

[22] Chao, C., et al, "Challenges and Options for GEO Use of GPS," AAS 97-677, AAS/AIAA Astrodynamics Specialist Conference, August 1997, pp. 1171-1183.

[23] Powell, T., Menn, M., Feess, W., "Evaluation of GPS Architecture for High Altitude Spaceborne Users," *Proceedings of the 54th Annual Meeting of The Institute of Navigation*, June 1998, pp 157-165.

[24] Kronman, J., "Experience Using GPS For Orbit Determination of a Geosynchronous Satellite," *Proceedings of the Institute of Navigation GPS 2000 Conference*, Sept. 2000, pp. 1622-1626.

[25] Ruiz, J., Frey, C., "Geosynchronous Satellite Use of GPS," *Proceedings of the Institute of Navigation GNSS 2005 Conference*, Sept. 2005, pp. 1227-1232.

[26] Bamford, B., Winternitz, L., Moreau, M., "Real-Time Geostationary Orbit Determination Using the Navigator GPS Receiver," 2005 Flight Mechanics Symposium, Oct. 2005.

[27] Bamford, W., Naasz, B., Moreau, M., "Navigation Performance in High Earth Orbits using Navigator GPS Receiver," AAS-06-045, *Advances in the Astronautical Sciences, Guidance and Control 2006*, Vol. 125, Feb. 2006, pp. 261-276.

[28] Barker, L., "GPS Beyond LEO: Signal Environment System Design Considerations," AAS-08-003, *Advances in the Astronautical Sciences, Guidance and Control 2008*, Vol. 131, Feb. 2008, pp. 31-48.

[29] Barker, L., and Frey, C., "GPS at GEO - SBIRS GEO1 First Look," AAS 12-044, *Advances in the Astronautical*

Sciences, Guidance and Control 2012, Vol. 144, Feb. 2012, pp. 199-212.

[30] Burkert, J., Frey, C., Mottinger, B., "GPS Navigation at GEO," Lockheed Martin Joint Technical Focus Group Conference, Apr. 2012.

[31] Gleason, et al, "Calibration and Unwrapping of the Normalized Scattering Cross Section for the Cyclone Global Navigation Satellite System," *IEEE Transactions on Geoscience and Remote Sensing*, VOL. 54, NO. 5, MAY 2016.

[32] Larson, K., and Gaylor, D., Winkler, S., "GOES-R Worst-Case GPS Constellation For Testing Navigation At Geosynchronous Orbit," AAS 13-064, *Advances in the Astronautical Sciences, Guidance and Control 2013*, Vol. 149, Feb. 2013, pp. 403-416.

[33] Balbach, O., et al, "Tracking GPS Above GPS Satellite Altitude: Results of the GPS Experiment on the HEO Mission Equator-S," *Proceedings of the Institute of Navigation GPS 1998 Conference*, Sept. 1998, pp. 1555-1564.

[34] Moreau, M., Axelrad, P., Garrison, J., Long, A., "GPS Receiver Architecture and Expected Performance for Autonomous Navigation in High Earth Orbits," *Navigation: Journal of The Institute of Navigation*, Vol. 47, No. 3, Fall 2000, pp. 191-204.

[35] Moreau, M., et al., "Results from the GPS Flight Experiment on the High Earth Orbit AMSAT OSCAR-40 Spacecraft," *Proceedings of the Institute of Navigation GPS 2002 Conference*, Sept. 2002, pp. 122-133.

[36] Bamford, W., Winternitz, L., and Hay, C., "Autonomous GPS Positioning at High Earth Orbits," *GPS World*, Vol. 17, No. 4, Apr. 2006, pp. 50-55.

[37] Carpenter, J., et al, "Libration Point Navigation Concepts Supporting the Vision for Space Exploration," AIAA-2004-4747, AAS/AIAA Astrodynamics Specialist Conference, Aug. 2004, pp. 319-338.

[38] Lee, T., et al, "Navigating the Return Trip from the Moon using Earth-Based Ground Tracking and GPS (AAS 09-056)," *Advances in the Astronautical Sciences, Guidance and Control 2009*, Vol. 133, Feb. 2009, pp. 319-338.

[39] Silva, P., et al, "Weak GNSS Signal Navigation to the Moon," *Proceedings of the Institute of Navigation GNSS 2013 Conference*, Sept. 2013, pp. 3357-3367.

[40] Farahmand, M., Long, A., Carpenter, R., "Magnetospheric MultiScale Mission Navigation Performance Using the Goddard Enhanced Onboard Navigation System," *Proceedings of the 25th International Symposium on Space Flight Dynamics*, www.issfd.org, 2015.

[41] Parker, J., Miller, J., private communication, July, 2016.

[42] Winkler, S., Voboril, C., Hart, R., King, M., "GOES-R Use of GPS at GEO," AAS 13-063, *Advances in the Astronautical Sciences, Guidance and Control 2013*, Vol. 149, Feb. 2013, pp. 391-402.

[43] Silva, P., et al, "GNSS-Based Navigation for Lunar Descent and Landing Performance Results," NAVITEC, 2014.

[44] Lopes, "GNSS-Based Navigation for Lunar Missions," ION-GNSS-2014.

[45] Montenbruck, O., private communication, July, 2016.

[46] Edgar, C., Goldstein, D., Bentley, P., "Current Constellation GPS Satellite Ground Received Signal Power Measurements," *Proceedings of the 2002 National Technical Meeting of The Institute of Navigation*, San Diego, CA, January 2002, pp. 948-954.

[47] Parker, J., Valdez, J., Bauer, F., Moreau, M., "Use and Protection of GPS Sidelobe Signals for Enhanced Navigation Performance in High Earth Orbit," 39th Annual AAS Guidance and Control Conference, Feb 5–10, 2016, Breckenridge, CO, AAS 16-72.

[48] Musumeci, L., et al, "Design of a High Sensitivity GNSS receiver for Lunar missions," Advances in Space Research journal, Mar. 2016, pp. 2285–2313.

[49] Axelrad, P, et al, "GEO Satellite Positioning Using GPS Collective Detection," ION-GNSS-2010.